HYDROLOGICAL PROCESSES
Hydrol. Process. **18**, 3667–3679 (2004)
Published online in Wiley InterScience (www.interscience.wiley.com). DOI: 10.1002/hyp.5794

The GEOTOP snow module

Fabrizio Zanotti, Stefano Endrizzi, Giacomo Bertoldi and Riccardo Rigon*
Department of Civil and Environmental Engineering CUDAM, Università di Trento, Trento, Italy

Abstract:

A snow accumulation and melt module implemented in the GEOTOP model is presented and tested. GEOTOP, a distributed model of the hydrological cycle, based on digital elevation models (DEMs), calculates the discharge at the basin outlet and estimates the local and distributed values of several hydro-meteorological quantities. It solves the energy and the mass balance jointly and deals accurately with the effects of topography on the interactions among radiation physics, energy balance and the hydrological cycle. Soil properties are considered to depend on soil temperature and moisture, and the heat and water transfer in the soil is modelled using a multilayer approach. The snow module solves for the soil–snow energy and mass exchanges, and, together with a runoff production module, is embedded in a more general energy balance model that provides all the boundary conditions required. The snowpack is schematized as a single snow layer where a limited number of physical processes are described. The module can be seen essentially as a parameter-free model. The application to an alpine catchment (Rio Valbiolo, Trentino, Italy), monitored by an *in situ* snow-depth sensor, is discussed and shown to give results comparable to those of more complex models. Copyright © 2004 John Wiley & Sons, Ltd.

KEY WORDS snow; snowmelt; distributed modelling; energy balance

INTRODUCTION

A suitable model of the hydrological cycle of mountain catchments and basins located at higher latitudes must account for snow accumulation and melting and for soil freezing. The presence of snow modifies the energy and mass balances, and snowmelt is responsible for most of the runoff during the melting season. Snowmelt processes have been modelled with different approaches of variable complexity, ranging from simple methods based only on temperature measurements (Morris, 1985) to complete multilayer models based on an energy balance (Marks *et al*., 1999), like the one-dimensional US Army Cold Regions Research and Engineering Laboratory Model (SNTHERM; Jordan, 1991). This model makes use of a mixture theory to describe all the dry air, dry soil and water phases dynamics and thermal constituents, and it requires a large number of snow layers to be set and short integration intervals for the simulations. SNTHERM is a reference for the description of point processes (Jin *et al*., 1999), but owing to its complexity it is not suited to direct implementation within a distributed model of the hydrological cycle. In fact, it neglects all those phenomena related to lateral flows and surface conditions whose accurate description could be more important than that of the local internal dynamics of the snow pack. An accurate treatment of radiation physics and its interaction with the mountain environment would be a necessary prerequisite to the use of the SNTHERM model.

Following SNTHERM, several models were developed, either as a direct simplification of it, like the SAST model (Jin *et al*., 1999; Sun *et al*., 1999), or through different approaches to the description of the energy balance (e.g. Blöschl *et al*., 1991a,b; Tarboton and Luce, 1996; Marks *et al*., 1999; Tuteja and Cunnane, 1999). Despite the lack of mathematical details, Blöschl *et al*. (1991a) gave a clear description of the features that a hydrologically sound model should have (including of a theoretical description of a proper treatment

* Correspondence to: Riccardo Rigon, Department of Civil and Environmental Engineering, CUDAM, Università di Trento, Trento, Italy.
E-mail: riccardo.rigon@ing.unitn.it

Received 12 April 2004
Accepted 27 September 2004

for the sky-view factor that the authors themselves did not pursue). Tarboton and Luce (1996) successfully implemented the Utah energy balance (UEB) model, although they neglected the interactions between the snow and all the other agents of the hydrological cycle. Tuteja and Cunnane (1999) presented a sound modelling approach, but the runoff module is treated with a lumped classical gamma-function-based model rather than a distributed one. All the above models can be referred to as 'high-resolution models' owing to the integration grid spatial scale, which is intended to be of the order of a few hundreds of square metres.

In parallel with the above-mentioned approaches, in the last 30 years many soil–atmosphere interaction models (also called land surface models, LSMs) have been developed that contain snow accumulation and melting modules, although mainly these are addressed to support of global circulation atmospheric models (GCMs) or meteorological modelling. Modern LSMs, like CLASS (Verseghy, 1991; Verseghy *et al*., 1993), BATS (Dickinson *et al*., 1986), or NCAR-LSM (Bonan, 1996), tend to represent soil–atmosphere vertical interactions with high degrees of physical complexity, but they are not endowed with a detailed representation of runoff and lateral fluxes. From this point of view (with the considerable exception of the VIC model (Liang *et al*., 1994), which, however, has a parameterized treatment of snow), they can be considered one-dimensional (vertical) models in which all the lateral hydrological fluxes occur only through the atmosphere. The grid size on which they operate is of the order of 1 km^2 to a few degrees in latitude and longitude, thus raising at least two questions: whether the physical dynamics implemented are sensible at this coarse scale and whether, vice versa, the test of the LSM schemes at a point (or with point measurements) should be considered useful for their validation.

In fact, most of the energy balance snowmelt modules of LSMs work fairly well at the point scale when the appropriate boundary conditions are set; nonetheless, they lead to considerably different quantitative results when compared in operational conditions (Jin *et al*., 1999). The main problems seem to be associated with the description of heat transfer processes in the stable atmospheric boundary layer and, to some extent, with a lack of parameterization of the processes and variability at the sub-grid scale. Fractional snow cover, snow albedo, and their interplay have a considerable effect on the energy available for ablation, with disagreement between models mostly evident at lower snow depths (Slater *et al*., 2001). Pomeroy *et al*. (2003) suggested that, at least in an alpine environment, elevation, aspect, and slope exert a major control on snow distribution, affecting snow accumulation, snowmelt energetics, the resulting meltwater fluxes and runoff contributing area, and that the scale of these processes (10–100 m) is much smaller than the grid resolution of most LSMs (10–100 km). Such effects cannot be explicitly described without a small-scale, physically based distributed model capable of taking in account both snow and hydrological processes involved in runoff production. Moreover, runoff production cannot be adequately described without a state-of-the-art treatment of the hydrological processes at hillslope and basin scale.

Despite the existence of (just) a few models that incorporate all the requirements outlined in Blöschl *et al*. (1991a) and Pomeroy *et al*. (2003)—for instance, the DHVSM model (Wigmosta *et al*., 1994), which has been applied to study snow melting in small mountain basins with remarkable results—we have implemented a new model for snow deposition, melting and ablation that also includes a physically based and fully distributed description of the hydrological processes of runoff production. This has been suggested by the reasons already discussed above and by the need to give a better insight into many ambiguous aspects of the numerical implementation of the existing models, as well as the parameterization of the sub-grid variability of the phenomena.

This model, GEOTOP (Bertoldi, 2004; Bertoldi *et al*., 2004; Rigon *et al*., unpublished results), can be seen both as a rainfall-runoff model, able to simulate the hydrological cycle in a continuous mode, and as an attempt to incorporate into LSMs an adequate treatment of hydrological variability at small scales (in particular, the effects due to different land uses, complex topography, and the channel network). Moreover, GEOTOP implements a consistent treatment of radiation and local atmospheric forcing that, it is believed, is critical to the successful development, testing and implementation of spatially distributed snow models (Marks *et al*., 1999; Susong *et al*., 1999).

AN OVERVIEW OF GEOTOP

The GEOTOP model is based on digital elevation models (DEMs), and it can make use of meteorological measurements obtained by traditional instruments as well as by distributed measurements from radar and satellite platforms or micro-meteorological models. Required forcing variables are precipitation, air temperature, pressure and humidity, and wind speed; optional variables to be used, if available, are shortwave global and diffuse radiation, longwave radiation, and cloud cover.

GEOTOP, like a rainfall-runoff model, calculates the discharge at the outlet of the watershed; moreover, it estimates the surface and subsurface water fluxes, the water table depth, and the value of the matric potential in both the saturated and the unsaturated portions of the soil mantle. Like an LSM, it estimates the local values and the spatial distribution of numerous hydro-meteorological variables, such as soil moisture, surface temperature, radiative fluxes, and heat fluxes into the soil. Furthermore, it simulates the evolution of the snow cover distribution.

Energy and mass conservation

The model solves the mass conservation equation for water:

$$\frac{\partial \theta}{\partial t} + \nabla \cdot \vec{Q} = 0 \tag{1}$$

and the equation for conservation of energy:

$$\frac{\partial U}{\partial t} + \nabla \cdot \vec{G} = 0 \tag{2}$$

where θ and U are respectively the water and internal energy content in the soil (or snow), $\vec{Q}$ and $\vec{G}$ are the water and the energy fluxes in the soil (or snow; considered to be vectors and positive if entering the control volume). Numerically integrating Equations (1) and (2) for each cell into which the watershed is divided and for the ith layer of snow/soil (i is the layer index, ranging from zero, at the surface, to the number of layers N, at the bottom), we obtain

$$\frac{\Delta \theta_i}{\Delta t} = Q_{i-1,i} - Q_{i,i+1} + Q_{\mathrm{h,in}} - Q_{\mathrm{h,out}} \tag{3}$$

and

$$\frac{\Delta U_i}{\Delta t} = G_{i-1,i} - G_{i,i+1} + G_{\mathrm{h,in}} - G_{\mathrm{h,out}} \tag{4}$$

where the fluxes of water $Q_{i-1,i}$ and $Q_{i,i+1}$ are respectively the vertical inflow from the layer above (or from the atmosphere for the superficial layer) and the vertical outflow towards the layer below. The heat fluxes $G_{i-1,i}$ and $G_{i,i+1}$ are defined analogously. A boundary condition on water (or heat) flux can be specified for the deepest layer. The fluxes $Q_{\mathrm{h,in}}$ and $Q_{\mathrm{h,out}}$ are the horizontal water inflow and outflow, and $G_{\mathrm{h,in}}$ and $G_{\mathrm{h,out}}$ are the lateral distributions of energy, which have been neglected, as they are usually much smaller than the vertical one.

The surface layer (of index $i = 0$) has infinitesimal thickness; it is a skin layer whose temperature is the surface temperature T_s. The first layer under the skin layer is the whole snowpack, if present, and can have any thickness. The other underlying layers are the soil layers.

The energy content U is divided between the energy of the soil component and energy of the water component (liquid or solid):

$$U = \chi_s U_s + \chi_w U_w \tag{5}$$

where χ_s and χ_w are respectively the dry soil and the water fractions, and U_s and U_w are the energy contents of these fractions. The value of U_s is relative to a reference state of soil at 0 °C and U_w to a reference state

of water in the ice (solid) phase ($U_w > 0$ means the water is in the liquid state or ice is isothermal with some liquid fraction, whereas when $U_w \leq 0$ only the solid phase is present). The energy content can then be used to calculate the layer average temperature and the liquid and solid components of the bi-phase snowpack.

The terms $Q_{i-1,i}$, $Q_{i,i+1}$, $Q_{h,in}$, and $Q_{h,out}$ (both vertical and horizontal fluxes between adjacent cells) in Equation (3) are evaluated by numerically solving the Richards equation (Richards, 1931). The terms $G_{i-1,i}$ and $G_{i,i+1}$ in Equation (4) are calculated according to the heat conduction law. If snowpack is present, then the heat flux advected by the flow of melting snow is also considered. Soil thermal capacity and conductivity are dependent on water content and temperature. To calculate the soil hydraulic properties we make use of the van Genuchten (1980) model, where the soil retention parameters can be derived from the soil texture by means of the pedotransfer functions proposed by Vereecken *et al*. (1989). The hydraulic conductivity is expressed as a function of the water content as in Mualem (1976).

Surface boundary conditions

Boundary conditions are defined by the interactions with the atmosphere (above) and by a known expression for the vertical variation of temperature and water flux (bottom). For the skin layer, if snowpack is absent then Equations (3) and (4) are rewritten as

$$0 = P - \mathrm{ET} - R - Q_{0,1} \tag{6}$$

and

$$0 = R_n - H - \lambda \mathrm{ET} + G_p - G_{0,1} \tag{7}$$

where P is the precipitation, ET the evapotranspiration (or sublimation from snow), R the runoff, R_n the net radiation, H the sensible heat flux, λET the latent heat flux (λ is either the evaporation latent heat or the sublimation latent heat), and G_p the heat flux advected with the precipitation (i.e. its energy content with respect to the reference state, assuming its temperature to be equal to the air temperature). The variations of θ and U are negligible, as the layer has infinitesimal thickness. If a snowpack is present, then the R term in Equation (6) disappears, as runoff is supposed to occur at the bottom of the snowpack. Thus, the mass balance equation for the first layer (i.e. the snowpack) can be rewritten as

$$\frac{\Delta\theta_1}{\Delta t} = Q_{0,1} - Q_{1,2} - R \tag{8}$$

where $\Delta\theta_1$ is the snowpack volume variation, $Q_{0,1}$ is the net precipitation on the snowpack, and $Q_{1,2}$ is the snow melting water flux.

Precipitation P is partitioned into rain P_{rain} and snow P_{snow}, according only to the air temperature (US Army Corps of Engineers, 1956). The effect of canopy interception for different land-cover classes is taken into account.

Runoff R can occur either because the precipitation intensity is greater than the soil surface infiltration capacity or because the water table level reaches the soil surface from below. Runoff is routed according to a kinematic scheme (and Manning type of roughness), and its calculation also accounts for rill formation and the spatial heterogeneity of the roughness parameter. All the cells of the basin's DEM are classified as either channel or hillslope cells. The motion of the water reaching the channels is described by the convolution of the incoming discharge with the solution to the de Saint-Venant equation proposed by Rinaldo *et al*. (1991).

An accurate calculation of the net radiation is essential for a model working in complex terrain (Dubayah *et al*., 1990). Solar radiation geometry is treated in GEOTOP as in Iqbal (1983). The model contains all the corrections needed in order to characterize a complex topography, including the calculation of shadowing of surrounding mountains, expressed by a factor *sw*. The effects of topography on diffuse radiation can be expressed through the sky view factor V, a parameter indicating the sky fraction that is visible at every location in the watershed. The relevance of V for the radiative balance in snow-covered mountain areas has

been highlighted by Blöschl *et al*. (1991a). Thus, taking into account the effects of shadowing and of the sky view factor, the net radiation R_n (W m^{-2}) is expressed as

$$R_n = (sw\ R^{\downarrow}_{SW\ P} + VR^{\downarrow}_{SW\ D})(1 - Va) + V\varepsilon_s R^{\downarrow}_{LW} - V\varepsilon_s \sigma T_s^4 \tag{9}$$

where $R^{\downarrow}_{SW}$ (W m^{-2}) is the shortwave net radiation (the subscript P refers to the direct component and D to the diffuse component, which is not influenced by shadowing but is proportional to the sky view factor); a is the shortwave albedo; ε_s is the longwave soil (or snow) emissivity; σ is the Stefan–Boltzmann constant (equal to $5{\cdot}6704 \times 10^{-8}$ W m^{-2} K^{-4}); $R^{\downarrow}_{LW}$ is the incoming longwave radiation, calculated according to the method of Brutsaert (1975), which depends on air temperature, air humidity and cloud cover; the factor *sw* is zero or one if the point is respectively in shadow or not; and the factor V gives the fraction of sky free from obstacles and ranges from zero to one. The term $(1 - Va)$ accounts for the shortwave radiation reflected by the surfaces surrounding a point and the last two terms of Equation (9) are multiplied by V to account for the longwave radiation emitted by the surfaces surrounding a point, under the hypothesis of radiative equilibrium.

Sensible H and latent λ ET heat fluxes are determined by the usual flux-gradient turbulent exchange relations (Garratt, 1992). GEOTOP also includes canopy transpiration and evaporation. Turbulent exchange coefficients are calculated according to similarity theory, and Louis (1979) theory is used to describe atmospheric stability as a function of the Richardson number.

For snow-covered surfaces, the latent heat flux is given by

$$(\lambda \mathrm{ET})_{snow} = uC_H \frac{h_v 0{\cdot}622}{R_d T_a}[e_a - e_{snow}(T_s)] \tag{10}$$

where u is the velocity of the wind, C_H is a turbulent transport coefficient, h_v the latent heat of ice vaporization, e_{snow} is the vapour pressure on the snow surface, assuming saturation at temperature T_s, calculated employing a polynomial approximation (Lowe, 1977), e_a is the vapour pressure in the air at the temperature T_a, and R_d is the universal gas constant for dry air.

The snow energy content

In the GEOTOP model, snow accumulation and melt are calculated following the UEB scheme (Tarboton and Luce, 1996). The UEB model is an energy-based one-layer snow model that is physically consistent but computationally efficient enough to be used in a basin-scale distributed model. In fact, the snowpack is characterized by three state variables: the snow water equivalent SWE (m), the energy content U (J m^{-2}), and the age of the snow surface (used only in the calculation of the albedo). The relations between the quantities related to the snowpack in the water and energy balance equations are reported in Table I.

The water and heat flux released by melting

The water flux released by the melting process is given by

$$Q_{1,2} = k_{sat}(S^*)^3 \qquad S^* = \frac{\text{liquid water volume} - \text{capillary retention}}{\text{pore volume} - \text{capillary retention}} \tag{11}$$

Table I. Temperature of the snowpack (T_1), and its liquid ($\chi_{w,liq}$) and solid ($\chi_{w,sol}$) content ρ_w and C_w are respectively the density and the specific heat of liquid water, C_{snow} is the specific heat of ice and h_f the latent heat of ice fusion

U	T_1 (snow)	$\chi_{w,sol}$	$\chi_{w,liq}$
≤ 0	$= \frac{U}{\rho_w\ \mathrm{SWE}\ C_{snow}} < 0\,^{\circ}\mathrm{C}$	1	0
>0; $\leq \rho_w$ SWE h_f	$= 0\,^{\circ}\mathrm{C}$	$1 - \frac{U}{\rho_w\ \mathrm{SWE}\ h_f}$	$\frac{U}{\rho_w\ \mathrm{SWE}\ h_f}$
$> \rho_w$ SWE h_f	$= \frac{U - \rho_w\ \mathrm{SWE}\ h_f}{\rho_w\ \mathrm{SWE}\ C_w} > 0\,^{\circ}\mathrm{C}$	0	1

where k_{sat} is the snow saturated hydraulic conductivity and S^* is the relative saturation in excess of water retained by capillary forces (Male and Gray, 1981: equation (9·45)). The melting latent heat is then

$$Q_m = \rho_w h_f Q_{1,2} \tag{12}$$

and contributes to the total heat flux $G_{1,2}$ in Equation (4).

For a complete description of the model, see Bertoldi *et al*. (2004).

A brief discussion

As derived from Equations (10) to (12) and from the heat conduction law, the only parameters involved in the description of the snow dynamics are the saturated hydraulic conductivity of the snow k_{sat}, the snow density ρ_{snow}, the snow specific heat C_{snow}, the snow thermal diffusivity k_{snow}, the air temperature below which the precipitation is only snow, and the parameters related to the calculation of S^* (the capillarity retention L_c) and of the albedo which are the bare ground albedo A_{bg}, the visible-band snow reflectance α_{vo}, the near-infrared band reflectance α_{iro}, and the albedo extinction depth AED, which is defined as the depth such that, when the snow depth is shallower than this depth, the albedo is interpolated between the snow value and bare ground value; see Tarboton and Luce (1996). The turbulent transport coefficient C_H depends on the roughness length z_0, often assumed as 1/10 of the canopy height. These parameters can be either calibrated to get a better agreement of the simulations with the measurements or assumed constant and equal to the values given in Table II. In the following simulations we chose to keep these parameters constant. In this sense, the snow module can be considered a parameter-free model.

Moreover, we remark that our model:

1. evaluates the heat fluxes internally (differently from the UEB model, which parameterizes them), in particular the heat exchanged with the soil;
2. routes and provides as input to the runoff and infiltration modules the water derived from snowmelt (in general, all the input fluxes of the UEB model are provided by the other modules of GEOTOP);

Table II. Snow parameters used in the GEOTOP simulation

Parameter	Value	Description	Reference
k_{sat}	0·00555	Snow saturated hydraulic conductivity (m s^{-1})	Tarboton and Luce (1996)
ρ_{snow}	350	Density of snow (kg m^{-3})	Measured data average value
C_{snow}	2090	Snow specific heat (J kg^{-1} K^{-1})	Tarboton and Luce (1996)
k_{snow}	$5{\cdot}55 \times 10^{-6}$	Snow thermal diffusivity (m^2 s^{-1})	Tarboton and Luce (1996)
$T_{thres,r}$	3	Temperature above which all precipitation is rain (°C)	US Army Corps of Engineers (1956)
$T_{thres,s}$	−1	Temperature below which all precipitation is snow (°C)	US Army Corps of Engineers (1956)
L_c	0·054	Liquid holding capacity of snow (dimensionless)	Tarboton and Luce (1996)
A_{bg}	0·2	Bare ground albedo (dimensionless)	Tarboton and Luce (1996)
α_{vo}	0·85	Snow visible-band reflectance (dimensionless)	Tarboton and Luce (1996)
α_{iro}	0·65	Snow near-infrared band reflectance (dimensionless)	Tarboton and Luce (1996)
AED	0·1	Albedo extinction depth (m)	Tarboton and Luce (1996)
W_{acc}	150·0	Mean water equivalent depth of snow (mm) at the beginning of the simulation of accumulation period	Measured data
W_{melt}	650·0	Mean water equivalent depth of snow (mm) at the beginning of the simulation of melting period	Measured data

3. takes into account the shadow and sky-view factors in calculating the radiation.

STUDY SITE AND MODEL RESULTS

The area analysed is the Rio Valbiolo basin, which is shown in Figure 1, and is located close to Tonale Pass in the Alps, in Trentino (Italy). Its area is 12 km^2 and its elevation ranges between 1600 and 2900 m above sea level. The model has been forced with the data supplied by the Tonale measurement station belonging to the meteorological office of the local government of Trentino, located at 1880 m above sea level inside the Rio Valbiolo basin.

The data provided are:

- Meteorological data measured every 15 min, for two periods, from 8 November 2000 to 13 March 2001 and from 7 April 2001 to 21 May 2001, i.e. precipitation, air temperature, relative humidity, pressure, wind speed and global shortwave radiation.
- Weekly snow stratigraphy data obtained by A.I.Ne.Va (Associazione Interregionale Neve e Valanghe, i.e. Snow and Avalanches Interregional Association, which groups the meteorological offices of some local governments) from 12 December 2000 to 18 April 2001.
- Daily snow depth data from 8 November 2000 to 21 May 2001.

The data have a gap between 14 March 2001 and 6 April 2001, due to instrumental damage. For this reason the simulation has been split in two parts: the first one during the snow accumulation period and the second one during the melting period.

For each weekly stratigraphic profile an average snow density has been calculated, and this value has been used to calculate the SWE from daily snow depth measurements, in order to obtain a continuous time series of SWE.

Atmospheric pressure and air temperature have been corrected for elevation under the assumption of neutral stability ($-0{\cdot}65\,^{\circ}C/100$ m for temperature and -11 hPa/100 m for pressure). Given the availability of data from only a single measurement station, no spatial interpolation scheme has been applied to precipitation and wind speed data.

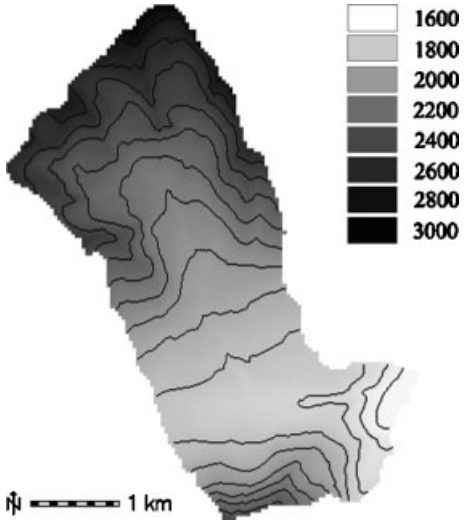

Figure 1. DEM of Rio Valbiolo catchment. Elevations are in metres

Local results at Tonale station

The parameters used in the simulations are summarized in Table II. A soil profile of four layers was set up with thickness values of (going from the top to the bottom) 0·2, 0·4, 1, and 2 m.

Figure 2 shows the comparison between SWE simulated with GEOTOP and SWE derived from the measurements. The model reproduces the local snow accumulation well, except for the snow-cover peaks following precipitation events. However, recent snow has much lower density than older snow; therefore, the assumption of a uniform snow density profile to calculate SWE from daily snow depth measurement gives an overestimation of the measured SWE immediately after snowfall. Using different values of snow density in the model does not change results significantly: a change in snow density from 200 to 500 kg m^{-3} results in an SWE change of less than 3%. The melting period is also well reproduced, with a small delay at the end of the season.

The effects of slope and aspect are highlighted in Figure 3, where the temporal evolution of the SWE is plotted for sites with different slope and aspect, but with the same elevation. At the end of the season, steep north-facing slopes are still increasing in SWE, whereas in steep south-facing slopes the snow cover is much more shallow (45% slope) or nearly absent (100% slope) for most of the season, with immediate melting after snowfall. The strong delay of the melting process in north-facing slopes compared with south-facing slopes has also been observed by Pomeroy *et al*. (2003).

Figures 4 and 5 show some results in terms of energy fluxes. In particular, Figure 4 shows energy flux oscillations in the accumulation period during the winter season, and Figure 5 shows the energy flux oscillations in the melting period during the spring season. The only melting during the winter period is caused by heat advected by the rain. During spring, however, the melting heat flux oscillates according to the shortwave radiation, which provides most of the melting energy. The contribution of the sensible heat fluxes from the air are negligible.

Rio Valbiolo catchment results

The model should give credible quantitative results in other points of the basin as soon as the meteorological variables are consistently modelled for the whole basin. Figures 6 to 8 present the results of the simulation on the whole Rio Valbiolo catchment. Owing to the lack of spatially distributed measurements on the

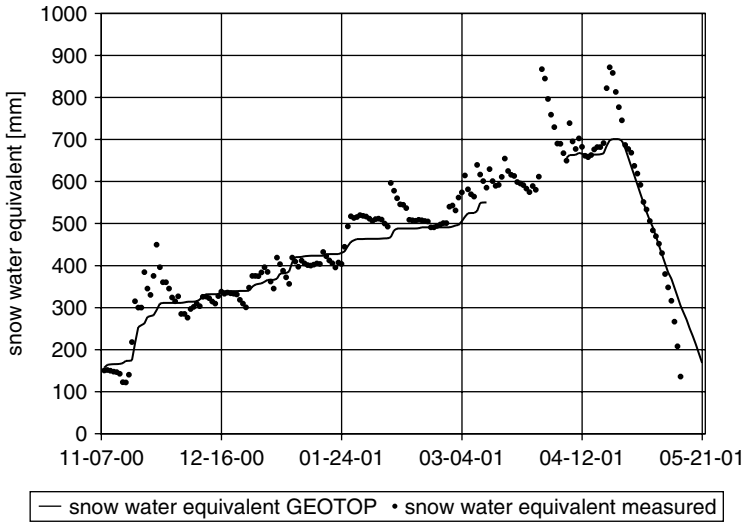

Figure 2. Simulated SWE at the meteorological station of Tonale pass (TN), compared with the measured SWE, 11 November 2000–21 May 2001

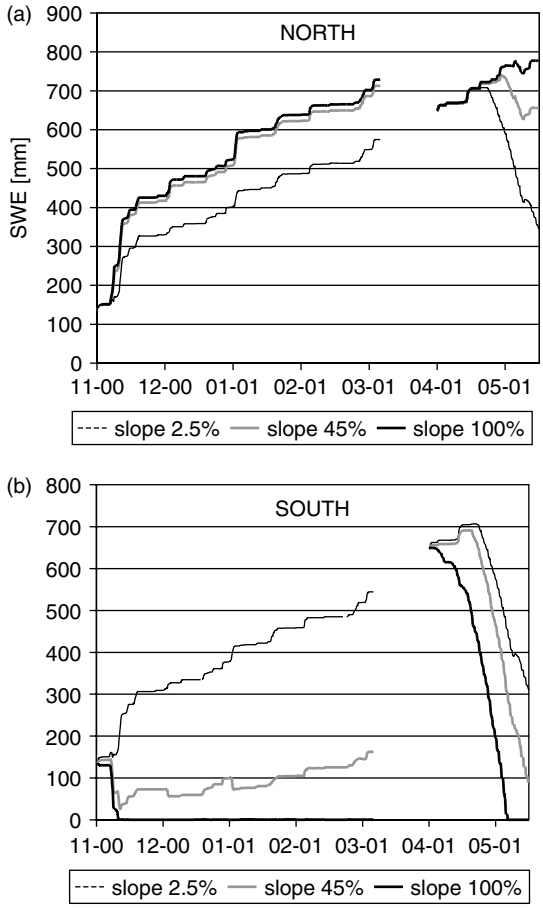

Figure 3. SWE evolution for sites with different slope and aspect; north and south aspects, 2·5, 45 and 100% slopes; separate simulations have been done for melting and accumulation seasons

catchment to compare against, the results are presented here just to demonstrate the soundness of our approach. The only source of spatial variability is topography; therefore, this case study can be useful to analyse how solar radiation distribution and elevation affect spatial patterns of SWE and total basin discharge.

Figure 6 shows the weekly averaged SWE distribution inside the basin for 2 weeks, during accumulation period and during melting period. SWE ranges between 150 and 800 mm. In the second map it is also possible to notice that north-facing slopes have more snow than south-facing slopes. The simulations of snow depth distribution show variability with elevation due mostly to temperature changes, but also related to aspect and different sky-view factors. Since the development of the clear-sky solar radiation model of Dozier (1980) the relevance of the terrain-reflected radiation in mountainous areas has been emphasised. Lower elevation sites receive less direct shortwave radiation but receive a considerable amount of longwave energy reflected from the surrounding mountain.

Figure 7 presents the weekly averaged surface temperature distributed over the basin. The snow surface temperature ranges between $-20\,^{\circ}\mathrm{C}$ (at higher elevations) and $0\,^{\circ}\mathrm{C}$. In the first map (January 2001) the whole snow surface is well below $0\,^{\circ}\mathrm{C}$, but the slope and aspect effects are well represented here: areas usually in shadow have significantly lower temperatures and negative surface fluxes, especially at the beginning of the

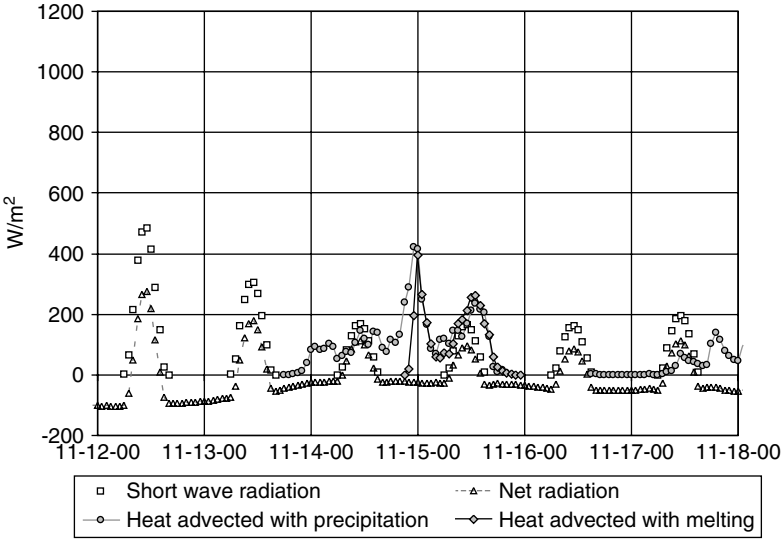

Figure 4. Simulated energy fluxes (a sample from the accumulation period) at the station, 12–18 November 2000

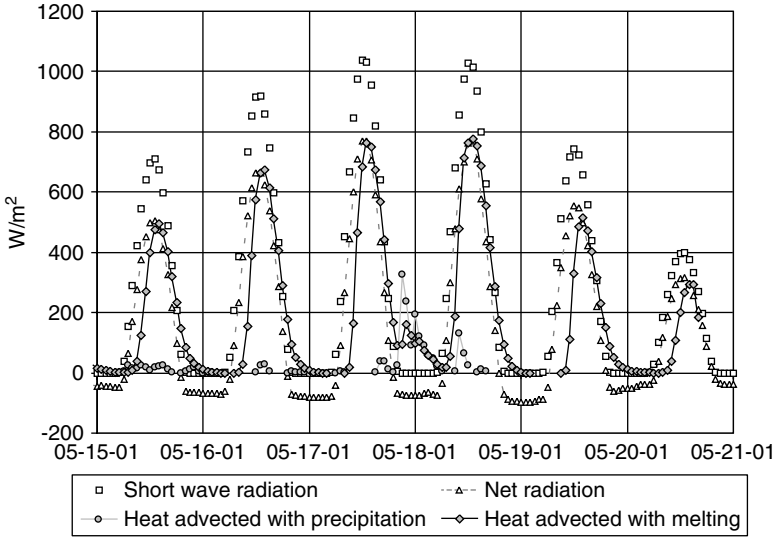

Figure 5. Simulated energy fluxes (a sample from the accumulation period) at the station, 15–25 May 2001

winter; on the contrary, during the late spring the spatial patterns of surface temperature are mainly correlated with elevation (April 2001). At the end of the spring (May 2001) the whole snow cover is in a melting condition and, therefore, is isothermal at 0 °C.

Runoff results

The water flux at the bottom of the snowpack $Q_{1,2}$ (both net precipitation and snow melting, see Equation (12)) is routed by the hydrological part of the model to the basin outlet. Figure 8 displays the mass balance of the basin during the melting period. The daily discharge is properly described, according to the snowmelt outflow. The runoff shows daily oscillations due to solar radiation. The liquid precipitation is

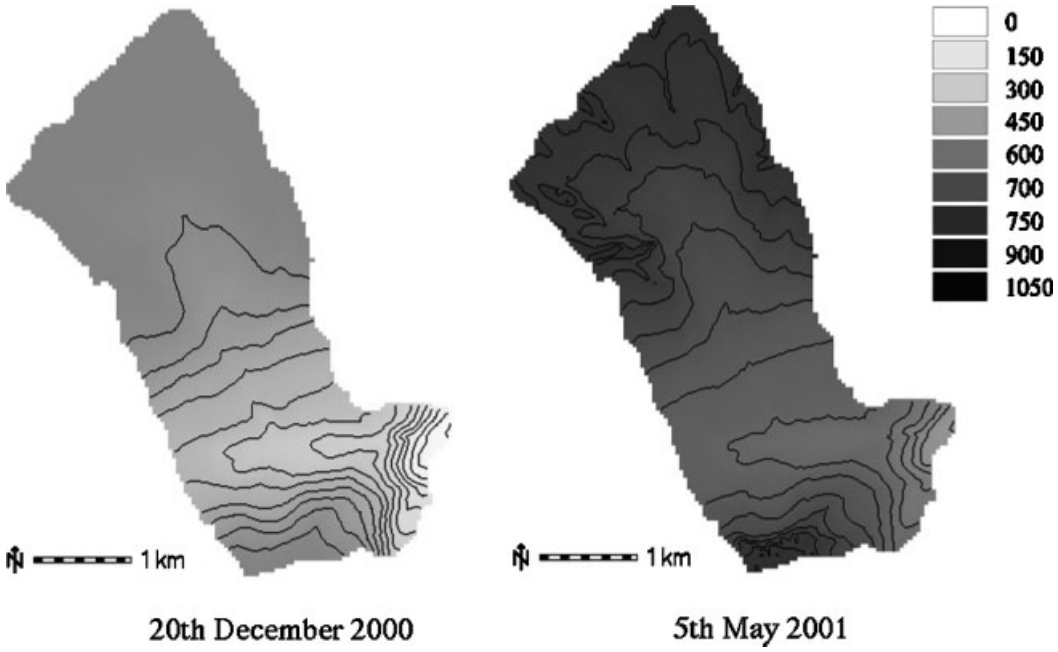

Figure 6. Map of SWE (mm, with contour lines at 25 mm intervals) for two characteristic weeks for the snow accumulation period (week beginning 20 December 2000) and snow melting period (week beginning 5 May 2001)

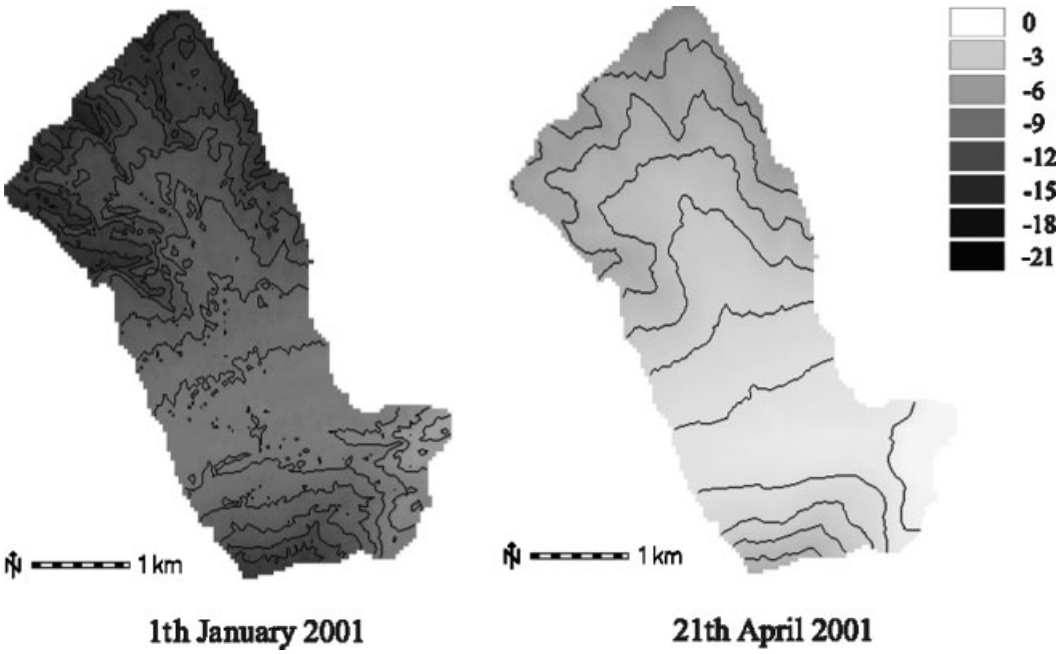

Figure 7. Map of surface temperature (°C, with contour lines at 1 °C intervals) for two characteristic days for the snow accumulation period (1 January 2001) and snow melting period (21 April 2001)

partially absorbed by the snowpack (20–21 April 2001) and partially released with the water outflow produced

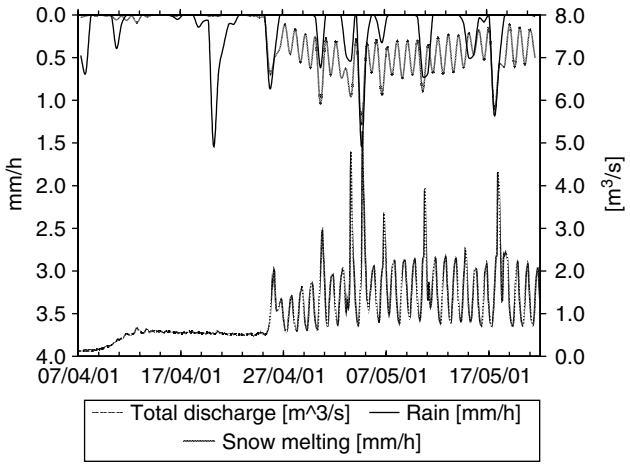

Figure 8. Mass balance overview during the snow melting period for the Rio Valbiolo catchment

by melting ($Q_{1,2}$) (from 26 April 2001). Discharge peaks are in correspondence with liquid precipitation events, but most of the runoff is given by snowmelt. This is in accordance with the findings of Blöschl *et al*. (1990). For a long simulation period, the dominance of shortwave radiation—though not as important during a single day event—indicates that topography should be considered.

CONCLUSION

The integration of the GEOTOP model with the snow module entails a better parameterization of the ground energy fluxes, and an accurate description of the snowmelt runoff and soil water storage. At the local scale, the model reproduces accurately the measured values without any calibration of snow parameters. However, the parameters of the energy balance, especially those related to turbulence exchange, can greatly affect the results. During the simulation those parameters were set according to values given in the literature. We focused mainly on the effects of topography and the partition of radiation and energy fluxes. Our simulations of the Rio Valbiolo catchment show that the model has the capability to account for the influence of the slope and aspect on the spatial distribution of the snow cover and for the effect of shadows on surface temperature. Moreover, it is able to reproduce discharge at the basin outlet at hourly time scales. This suggests that LSMs that do not parameterize the topography could give very erroneous results when applied.

ACKNOWLEDGEMENTS

We thank *Ufficio Neve Valanghe e Meteorologia*, Trento (Italy), for the data supplied, and the *MIUR*, which partially supports the research under the project PRIN2001: Interazione clima–suolo–vegetazione e suoi effetti sugli eventi meteorologici estremi (Climate–Soil–Vegetation interaction and effects on extreme meteorological events). We thank Thomas M. Over and Rocco Panciera for having read and commented on an early version of the manuscript.

REFERENCES

Bertoldi G. 2004. *The water and energy balance at basin scale: a distributed modelling approach*. University of Trento, Monograph of the School of Doctoral Studies in Environmental Engineering. http://www.ing.unitn.it/dica/eng/monographs/index.php (15 September 2004).

Bertoldi G, Tamanini D, Zanotti F, Rigon R. 2004. *GEOTOP: a hydrological balance model. Technical description and programs guide*. University of Trento (Italy) E-Prints. http://eprints.biblio.unitn.it/archive/00000551/ (4 April 2004)
Blöschl G, Kirnbauer R, Gutknecht D. 1990. Modelling snowmelt in a mountainous river basin on a event basis. *Journal of Hydrology* **113**: 207–229.
Blöschl G, Kirnbauer R, Gutknecht D. 1991a. Distributed snowmelt simulations in an alpine catchment 1. Model evaluation on the basis of snow cover patterns. *Water Resources Research* **27**(12): 3171–3179.
Blöschl G, Gutknecht D, Kirnbauer R. 1991b. Distributed snowmelt simulations in an alpine catchment 2. Parameter study and model predictions. *Water Resources Research* **27**(12): 3181–3188.
Bonan GB. 1996. *A land surface model for ecological, hydrological, and atmospheric studies: technical description and user's guide*. Technical Note NCAR/TN-417+STR. NCAR, Boulder, CO, USA.
Brutsaert W. 1975. On a derivable formula for long-wave radiation from clear skies. *Water Resources Research* **11**(5): 742–744.
Dickinson RE, Heanderson-Sellers A, Kennedy PJ, Wilson M. 1986. *Biosphere atmosphere transfer scheme (BATS) for the NCAR community climate model*. Technical Note NCAR/TN-275+STR. NCAR, Boulder, CO, USA.
Dozier J. 1980. A clear-sky spectral solar radiation model for snow-covered mountainous terrain. *Water Resources Research* **16**(4): 709–718.
Dubayah A, Dozier J, Davis F. 1990. Topographic distribution of clear-sky radiation over the Konza Prairie, Kansas. *Water Resources Research* **26**(4): 679–690.
Garratt JR. 1992. *The Atmospheric Boundary Layer*. Cambridge University Press.
Iqbal M. 1983. *An Introduction to Solar Radiation*. Academic Press.
Jin J, Gao X, Yang ZL, Bales RC, Sorooshian S, Dickinson RE, Sun SF, Wu GX. 1999. Comparative analyses of physically based snowmelt models for climate simulations. *Journal of Climate* **12**: 2643–2657.
Jordan R. 1991. *A one-dimensional temperature model for a snowcover: technical documentation for SNTHERM 89, Spec. Rep. 657, user's guide*. US Army Cold Regions Research and Engineering Laboratory, Hanover, NH.
Kitanidis PK. 1997. *Introduction to Geostatistic Application in Hydrogeology*. Cambridge University Press.
Liang X, Lettenmaier DP, Wood EF, Burges SJ. 1994. A simple hydrologically based model of land surface water and energy fluxes for general circulation models. *Journal of Geophysical Research* **99**(D7): 14 415–14 428.
Louis JF. 1979. A parametric model of vertical eddy fluxes in the atmosphere. *Boundary Layer Meteorology* **17**: 187–202.
Lowe PR. 1977. An approximating polynomial for the computation of saturation vapour pressure. *Journal of Applied Meteorology* **16**: 100–103.
Male DH, Gray DM. 1981. *Handbook of Snow, Principles, Processes, Management and Use*. Pergamon Press.
Marks D, Domingo J, Susong D, Link T, Garen D. 1999. A spatially distributed energy balance snowmelt model for application in mountain basins. *Hydrological Processes* **13**: 1935–1959.
Morris EM. 1985. Snow and ice. In *Hydrological Forecasting*, Anderson MG, Burt TP (eds). John Wiley: 153–182.
Mualem Y. 1976. A new model for predicting the hydraulic conductivity of unsaturated porous media. *Water Resources Research* **12**: 513–522.
Pomeroy JW, Toth B, Granger RJ, Hedstrom NR, Essery RLH. 2003. Variation in surface energetics during snowmelt in a subarctic mountain catchment. *Journal of Hydrometeorology* **4**(4): 702–719.
Richards LA. 1931. Capillary conduction of liquids in porous mediums. *Physics* **1**: 318–333.
Rinaldo A, Marani A, Rigon R. Geomorphological dispersion. 1991. *Water Resources Research* **27**(4): 513–525.
Slater AG, Schlosser CA, Desborough CE, Pitman AJ, Henderson-Sellers A, Robock A, Vinnikov KYa, Mitchell K, Boone A, Braden H, Chen F, Cox PM, de Rosnay P, Dickinson RE, Dai YJ, Duan Q, Entin J, Etchevers P, Gedney N, Gusev YM, Habets F, Kim J, Koren V, Kowalczyk EA, Nasonova ON, Noilhan J, Schaake S, Shmakin AB, Smirnova TG, Verseghy D, Wetzel P, Xue Y, Yang ZL, Zeng Q. 2001. The representation of snow in land surface schemes: results from PILPS 2(D). *Journal of Hydrometeorology* **2**: 7–25.
Sun SF, Jin J, Xue Y. 1999. A simple snow–atmospheric–soil transfer (SAST) model. *Journal of Geophysical Research* **104**: 19 587–19 598.
Susong D, Marks D, Garen D. 1999. Methods for developing time-series climate surfaces to drive topographically distributed energy and water balance models. *Hydrological Processes* **13**: 2003–2021.
Tarboton DG, Luce CH. 1996. *Utah energy balance snow accumulation and melt model (UEB). Computer model technical description and users guide*. Utah Water Research Laboratory, Utah State University and USDA Forest Service Intermountain Research Station.
Tuteja NK, Cunnane C. 1999. A quasi physical snowmelt runoff modelling system for small catchments. *Hydrological Processes* **13**: 1961–1975.
US Army Corps of Engineers. 1956. *Snow hydrology, Summary report of the snow investigations*. US Army Corps of Engineers, North Pacific Division, Portland, OR.
Van Genuchten MT. 1980. A closed-form equation for predicting the hydraulic conductivity of unsaturated soils. *Soil Science Society America Journal* **44**: 892–898.
Vereecken H, Maes J, Feyen J, Darius P. 1989. Estimating the soil moisture retention characteristic from texture, bulk density and carbon content. *Soil Science* **148**: 389–403.
Verseghy DL. 1991. CLASS—a Canadian land surface scheme for GCMS. Part I: soil model. *International Journal of Climatology* **11**: 111–133.
Verseghy DL, Mcfarlane NA, Lazare M. 1993. CLASS—a Canadian land surface scheme for GCMS. Part II: vegetation model and coupled runs. *International Journal of Climatology* **3**: 347–370.
Wigmosta MS, Vail L, Lettenmaier D. 1994. A distributed hydrology–vegetation model for complex terrain. *Water Resources Research* **30**(6): 1665–1679.

